Age-linked heterogeneity among oligodendrocyte precursor cells in the cerebral cortex of mice and human

Authors: Bribián A[1,2], Medina-Rodríguez EM [1,7], Josa-Prado F[2], García-Álvarez I[1,3], Machín-Díaz I[1], Murcia-Belmonte V[1,4], Vega-Zelaya L[5], Pastor J[5], Garrido L[6] and de Castro, F[1,2]

[1]Hospital Nacional de Parapléjicos, Finca "La Peraleda" s/n, 45071 Toledo, Spain.
[2]Instituto Cajal-CSIC, Avda. Dr. Arce 37,28002 Madrid, Spain.
[3]Institutode Química Orgánica General (IQOG-CSIC), CSIC, Juan de la Cierva 3, 28006 Madrid, Spain.
[4]Instituto de Neurociencias, Universidad Miguel Hernández-CSIC, Campus San Juan de Alicante, 03550 Alicante, Spain.
[5]Neurofisiología Clínica; Instituto de Investigación Sanitaria, Hospital Universitario de la Princesa, Madrid, Spain.
[6]Instituto de Ciencia y Tecnología de Polímeros (ICTP-CSIC), CSIC, Juan de la Cierva 3, 28006 Madrid, Spain.
[7]University of Miami, Coral Gables, FL 33124, USA.

Corresponding author:

F. de Castro PhD, MD
Grupo de Neurobiología del Desarrollo-GNDe
Instituto Cajal-CSIC
Avda. Dr. Arce 37. 28002, Madrid, Spain.
Phone: 91-5854650
fdecastro@cajal.csic.es

ABSTRACT

Oligodendrocyte precursor cells (OPCs) are responsible for spontaneous remyelination after a demyelinating lesion. They are present in large parts of the mouse and human central nervous system, both during development and in adulthood, yet how their physiological behaviour is modified throughout life remains largely unknown. Moreover, the activity of adult human OPCs is still not fully understood. Significantly, most of the molecules involved in OPC-mediated remyelination are also involved in their development, a phenomenon that may be clinically relevant. In this article, we have systematically analyzed the intrinsic properties of OPCs isolated from the cerebral cortex of neonatal, postnatal and adult mice, as well as those recovered from neurosurgical adult human cerebral cortex tissue. We also analyze the response of these cells to two molecules that have known effects on OPC biology during development and that are overexpressed in individuals with Multiple Sclerosis (MS): FGF2 and anosmin-1. By analyzing intact OPCs for the first time with H-1 HR-MAS NMR spectroscopy, we show that these cells behave distinctly and that they have different metabolic patterns in function of their stage of maturity. Moreover, their response to FGF-2 and anosmin-1 differs in relation to their developmental stage and in function of the species. Our data reveal that the behaviour of adult human and mouse OPCs differs in a very dynamic way that should be considered when testing drugs and for the proper design of effective pharmacological and/or cell therapies for MS.

KEYWORDS

oligodendrocyte, myelin, Multiple Sclerosis, human, remyelination.

ABBREVIATIONS

CNS: Central nervous system

DMEM: Dulbecco's Modified Eagle's Medium

ECM: extracellular matrix

FBS: Fetal Bovine Serum

HRMAS: high-resolution magic angle spinning

MS: Multiple Sclerosis

OPC: Oligodendrocyte precursor cell

INTRODUCTION

Oligodendrocyte precursor cells (OPCs) are the sole source of oligodendrocytes, the myelin-forming cells in the central nervous system (CNS), and they are widely distributed throughout both the gray and white matter [1-5]. The vast majority of mature oligodendrocytes are born during postnatal life but in adults, oligodendrocytes can also be generated from OPCs that continue to divide and generate new-myelinating cells during adulthood [5-11]. In the adult brain, OPCs constitute 2–3% of the cells inthe gray matter and 5–8% in the white matter [1]. These cells are maintained as a resident population by self-renewal, representing the main proliferative cell type outside the neurogenic regions of the CNS [1,7,12,13]. However, the adult OPC population is not homogeneous as OPCs cycle less intensely with age, their proliferation rate is higher in the whiter matter than in the grey matter, and their differentiation rate declines progressively in postnatal and adult life [1,5,8-11,14,15]. Although the functions of adult-born oligodendrocytes remain largely unclear, they apparently maintain physiological oligodendroglial homeostasis and under pathological circumstances, they mediate long-term repair in the white matter after injury and disease, even in MS where they can partially restore the lost myelin sheaths [16,17]. In demyelinating diseases, there is an up-regulation of different molecules in the microenvironment in and around the lesions, including several factors that are important for developmental oligodendrogliogenesis, such as secreted semaphorins, growth factors, mitogens and adhesion molecules [18-24].

In the present study, we focused on cerebral cortex OPCs to avoid any variability introduced by anatomical origin or location. We examined the degree of intrinsic heterogeneity (both heterochronic and interspecies) of these cortical OPCs and we described the dynamic changes in their intrinsic properties when assessed by NMR (i.e, metabolic patterns), and how these changes affect their response to two molecules known to influence OPC biology during development and remyelination: FGF2 and anosmin-1 [19,25-33]. We systematically studied mouse cortical OPCs at different ages and OPCs isolated from the human adult cerebral cortex obtained from neurosurgery biopsies (resection margins of tumors and/or epilepsy surgery [34]). In terms of the latter, the scarcity of articles dealing with human OPCs is especially remarkable [21,34-38].

The data we obtained highlight the intrinsic physiological differences between mouse OPCs isolated at different ages. Indeed, while OPC proliferation and migration were enhanced similarly by FGF2, this factor produced different effects on OPC differentiation. By contrast, anosmin-1 elicited diverse effects on differentiating, and especially on migrating OPCs, yet not on the proliferation of these cells. While FGF2 was a chemoattractant for human and murine OPCs, anosmin-1 only attracted tumor-related cells and it repelled non-tumor OPCs. Neither FGF2 nor anosmin-1 affected human adult OPC differentiation. These observations confirm the chronological and inter-species heterogeneity of OPCs, adversity that will probably be relevant when designing effective pharmacological and/or cell therapies to repair myelin loss in MS and other demyelinating diseases.

103 **MATERIALS AND METHODS**

104 **Animals**

105 CD-1 mice were obtained from (Charles River Laboratories, Inc., Wilmington, MA) and
106 maintained in the animal facilities of the Hospital Nacional de Parapléjicos (Toledo,
107 Spain). OPCs were obtained from different age animals: embryonic (E16); postnatal
108 (P0, P7, P15); and adult (P60). All experimental procedures were carried out in
109 accordance with Spanish (RD223/88) and European (2010/63/EU) guidelines, and were
110 approved by the Animal Review Board at the Hospital Nacional de Parapléjicos
111 (SAPA001).

112 **Human biopsies**

113 Biopsies of human tumor (resection of the safety margins but not the tumor itself) and
114 non-tumor tissue (epilepsy surgery) were obtained from the Neurosurgery Service at the
115 Hospital La Princesa (Madrid, Spain). All human samples were obtained from the adult
116 brain cortex and the biopsies were predominantly from the temporal lobe (Table 1).
117 They were transported at 4°C as rapidly as possible in AQIX® RS-I (AQIX Ltd.,
118 Imperial College BioIncubator) to reduce cell damage. All experiments involving
119 human samples were carried out in accordance with the guidelines of the Research
120 Ethics Committee of our institution, which approved our research, and all the subjects
121 provided their written informed consent.

122 **HOG cells**

123 An immortalized oligodendroglioma cell line, HOG, was grown at 37ºC in an
124 atmosphere of 5% CO_2, and in Dulbecco's Modified Eagle's Medium (DMEM, Gibco)
125 supplemented with 10% Fetal Bovine Serum (FBS, Gibco), 100 U/mL penicillin and
126 100 µg/mL streptomycin (Sigma).

127 **Oligodendrocyte culture**

128 OPCs were isolated as described previously [19,34,38]. Briefly, the cerebral cortex of
129 mice aged E16, P0, P7, P15 and P60 was dissected out and the meninges were carefully
130 removed. The cortical tissue was mechanically disaggregated and it was then
131 enzymatically dissociated in a papain solution, filtered using a 100 µm nylon mesh
132 strainer (BD Biosciences), and seeded in polyornithine-treated flasks in DMEM

133 containing 10% FBS (BioWhittaker) and an antibiotic anti-mycotic solution (100 U/mL
134 penicillin/0.1 mg/mL streptomycin and 0.25 µg/ml Amphotericin B; Sigma). The
135 cultures were maintained at 37°C and in 5%CO_2, and the medium was changed every 4
136 days, adding10 ng/ml of human PDGF-AA (Millipore) to the cultures from adult mice.
137 When the cultures reached confluence, they were shaken overnight at 250 rpm to detach
138 the oligodendrocyte progenitors growing on the top of the confluent astrocyte
139 monolayer. The medium was then filtered through a 40µm nylon mesh strainer (BD
140 Biosciences) and centrifuged at 900 rpm. The cells recovered were seeded twice (45
141 minutes each) in bacterial grade Petri dishes (Sterilin) to remove the adherent microglia
142 and after another round of centrifugation, the resulting pellet was resuspended and the
143 OPCs were counted and seeded.

144 For cells obtained from human biopsies, the same protocol was used with certain
145 modifications published previously [34]. This protocol allowed us to obtain sufficient
146 human OPCs to perform the necessary assays. Briefly, rather than 75 cm^2flasks, 25 cm^2
147 flasks were used with a final volume of 5 ml rather than 10 ml OPC medium per flask.
148 In addition, the medium was supplemented with 10 ng/ml of human PDGF-AA
149 (Millipore), as in the cultures obtained from adult mice. Cultures reached confluence
150 after 30-40 days and the flasks were shaken at 230 rpm instead of 250 rpm.

151 **Preparation of extracts for anosmin-1**

152 Proteins from the extracellular matrix (ECM) of CHO cells (CT) and CHO cells stably
153 transfected with an expression plasmid carrying a C-terminal hemaglutinin-tagged (HA)
154 version of the human KAL1 cDNA (A1 [39]) were extracted as described previously
155 [32]. Briefly, the cells were washed once with calcium/magnesium-free Hank's
156 Balanced Salt Solution (Gibco) and they were then incubated at 4ºC for 30 minutes in a
157 gently rocking 10 cm diameter culture dish in 1 ml of 20 mM phosphate buffer (PB, pH
158 7.4), containing 350 mM NaCl and complete EDTA free protease inhibitor (Roche).
159 The ECM proteins released into the buffer were concentrated ten-fold with Amicon
160 Ultra-4 Ultracel-30k (Millipore Corporation) and used in the chemotaxis experiments
161 (ECM extracts). The presence of anosmin-1 was confirmed in western blots probed with
162 a peroxidase-conjugated rat monoclonal antibody against HA (High Affinity 3F10;
163 Roche). Equal amounts of protein from untransfected and transfected cells were used in
164 all the *in vitro* experiments described below.

165 **Chemotaxis**

166 To test chemoattraction, cells (murine and human OPCs, and HOG cells) were seeded in
167 the upper chamber of a chemotaxis chamber (40,000 cells/transwell), and FGF2
168 (20ng/ml; R&D Systems) or 0.1 mg/ml of CT and A1 cell extracts (see below) were
169 added to the lower chamber in Bottenstein-Sato (BS) medium, as reported previously
170 [19,27,32,40]. After 20 hours at 37ºC, the cells were fixed in 4% paraformaldehyde
171 (PFA) for 10 minutes at room temperature and the OPCs were stained with antibodies
172 against Ganglioside GT3 (A2B5, 1:20; Developmental Studies Hybridoma Bank) and
173 the Olig-2 oligodendroglial transcription factor (1:200, Millipore), and HOG cells were
174 stained with Hoechst. After immunostaining, the filters were examined using an In Cell
175 Analyzer 1000 (GE-HealthCare) and 15-20 microphotographs from each membrane
176 were taken randomly. The In Cell Analyzer 1000 Work station software was used (GE-
177 HealthCare) to quantify the number of transmigrated OPCs per field, expressing the
178 data as the percentage of migrating OPCs relative to the controls±s.e.m. (Considered as
179 100% [32]). The data were analyzed with the Sigma Stat software package (SPSS).

180 **Time-Lapse Imaging**

181 For a detailed study of OPC migration, time-lapse video-microscopy (Leica, DMI
182 6000B) was performed to observe the behaviour of the cortical OPCs. Purified OPCs
183 were placed on poly-L-lysine and laminin coated coverslips (10,000 cells/coverslip;
184 Sigma) and FGF2 (20ng/ml; R&D Systems) or CT CHO or A1-expressing CHO cell
185 extracts (0.1 mg/ml, see above) were added in BS medium. Images were taken every 20
186 minutes for 18 hours and the speed of cell motility was assessed with the manual
187 tracking plugin of the ImageJ software. The values represent the percentage of the mean
188 velocity relative to the respective controls (± s.e.m.).

189 **Differentiation assay**

190 Purified OPCs were placed on coverslips coated with poly-L-lysine and laminin (20,000
191 cells/coverslip), and FGF2 (20ng/ml; R&D Systems) or total protein from CT CHO
192 cells or A1-expressing CHO cells (0.1 mg/ml,see above) were added in differentiation
193 medium (BME:F12 media [1:1] supplemented with 100 μg/ml transferrin, 20 μg/ml
194 putrescine, 12.8 ng/ml progesterone, 10.4 ng/ml selenium, 25 μg/ml insulin, 0.8 μg/ml
195 thyroxine, 0.6% glucose, and 6.6 mM glutamine, as reported previously [34,38,41].

196 AraC (5µM; Sigma-Aldrich) was added to the cultures to inhibit proliferation and after
197 5-7days *in vitro* (DIV), the cells were fixed for immunocytochemical detection of
198 CNPase (1:200; Covance) and Olig-2 (1:200; Millipore). Finally, 10 random fields per
199 coverslip were photographed under a Leica microscope using a20X objective and the
200 proportion of $CNPase^+$ cells was assessed relative to the respective controls (± s.e.m.).

201 **Pharmacological treatments**

202 In order to study the mechanism underlying the activity of the FGF2/FGFR1/anosmin-1
203 system in specific aspects of cortical OPC biology (chemoattraction, motogenicity,
204 proliferation and differentiation), these processes were analyzed in the presence of the
205 specific FGFR inhibitor SU5402 [19,27,32,40]. The SU5402 inhibitor was reconstituted
206 in DMSO and the controls were administered the vehicle alone at the same
207 concentration to account for any negative effects of DMSO on OPCs.

208 **Differential FGFR expression**

209 FGFR1 expression in murine and human OPCs was assessed by dual
210 immunofluorescence with the OPC marker NG2 (1:200; Millipore) and an antibody
211 against FGFR1 (1:200; Santa Cruz Biotechnology). In order to understand the response
212 to FGF2 and anosmin-1 observed in OPCs from different ages, we studied the
213 expression of different FGFRs: FGFR1, FGFR2 and FGFR3. Cells were plated in 96-
214 well tissue culture plates (10,000 cells/well) and maintained at 37°C in a 5% CO_2
215 atmosphere and with 95% relative humidity in BS medium. After 1 DIV, the cells were
216 fixed for 10 min at room temperature with 4% PFA. The OPCs were immunostained
217 with antibodies against FGFR1 (1:200; Santa Cruz Biotechnology), FGFR2 (1:50; Santa
218 Cruz Biotechnology) and FGFR3 (1:20; Santa Cruz Biotechnology), and against tubulin
219 (1:40,000; Sigma-Aldrich). Antibody binding was detected using 680 or 800 IRDye
220 conjugated secondary antibodies and the plates were scanned using the Odyssey
221 Infrared Imaging System (LICOR). Fluorescence intensity was measured according to
222 the manufacturer's instructions and the amount of FGFRs relative to the amount of
223 tubulin was normalized to the FGFR expression in P0 samples. The values represent the
224 mean (± s.e.m.).

225 **Proliferation assays**

226 Purified OPCs were seeded on poly-L-lysine and laminin coated coverslips (20,000
227 cells/coverslip), and FGF2 (20ng/ml; R&D Systems) or CT CHO or A1-expressing
228 CHO cell extracts (0.1 mg/ml, see above) were added in BS medium. After 42 hours in
229 culture, a BrdU pulse (6 hours) was administered and 24 hours later, the cells were fixed
230 for immunocytochemical detection of BrdU and Olig-2, as described previously [27].
231 Finally, 10 random fields per coverslip were photographed under a Leica microscope
232 using a 20X objective and the data were expressed as the percentage of proliferating
233 OPCs relative to the controls (±s.e.m.) considered as 100%.

234 **H-1 HR-MAS NMR spectroscopy of OPCs**

235 H-1 HR-MAS NMR measurements were performed on a Bruker spectrometer operating
236 at 9.4 T (proton Larmor frequency of 400.14 MHz). The spectra were acquired at 4 ºC
237 to minimize the effect of temperature on cell stability during the acquisition time and to
238 reduce the variations in some amino acids [42]. Sample spinning at the magic angle was
239 applied at a speed of 2.4 kHz. The acquisition sequence and parameters were selected to
240 assess the presence of metabolites of interest and their mobility, essentially using T2-
241 filtered (CPMG) 1D experiments recorded with relaxation times of 2 and 60 ms. Low
242 power presaturation during the interscan delay of 3 s was applied for water suppression.
243 Typically, 256 scans were accumulated using a spectral width of 20 ppm, and the total
244 acquisition time per spectrum was 13 min.

245 The spectra were processed using MestReNova version 8.1 software (Mestrelab
246 Research, Santiago de Compostela, Spain) and all free induction decays were processed
247 with exponential multiplication (0.5 Hz line-broadening) prior to Fourier
248 transformation, followed by baseline correction. The chemical shifts were referenced as
249 follows: a small amount (5 mL) of 10 mM DSS in D_2O was added to one sample of
250 intact cells and referenced to DSS = 0 ppm, after which all the spectra were processed
251 identically and aligned (using the creatine methyl resonance at 3.026 ppm) with respect
252 to the sample with added DSS. Of the various methods to estimate or measure the
253 intensity of NMR signals [43], we compared peak intensity ratios using the methyl
254 signal of creatine as an internal reference. Creatine is commonly used as an internal
255 concentration reference for in vivo H-1 NMR because its concentration correlates with
256 the number of metabolically active cells and it can be used as a measure of viable cell
257 number [44]. Cells were washed (three times) with a deuterated PB solution,

258 centrifuged, and the cell pellet was frozen in liquid nitrogen and stored at -80 ºC.
259 Typically, approximately 60 µL of the cell pellet was placed into a 4 mm Ø zirconia
260 rotor for each sample.

261 **Imaging analysis**

262 Fluorescence digital images were obtained with a DFC480 FX digital camera (Leica)
263 coupled to a Leica DM5000 B microscope or using a SP5 resonant scanner (Leica
264 Microsystems).

265 **Statistical Analysis**

266 For all experimental conditions, the results were analyzed using a*t*-test (SigmaPlot 11
267 software (SPSS Science, Inc.) and critical values of: *P<0.05, **P<0.01 and
268 ***P<0.001.

269

RESULTS

Changes in the intrinsic properties of OPCs with aging

The intrinsic properties and metabolic pathways of murine OPCs isolated from the cerebral cortex were assessed at different ages (P0, P15 and P60). For the first time, we assessed these changes using H-1 high-resolution (HR)-magic angle spinning (MAS) NMR spectroscopy, which allows a large number of metabolites or small molecules in the cytoplasm to be systematically evaluated and their interaction with the local environment probed [45-47]. This approach may therefore provide valuable information on cellular physico-chemical characteristics that may be correlated with cellular processes of interest. We obtained 3 spectra for each group of OPCs, with two different echo-times TE ("T2 filters T2": 2, 10 and 60 ms), analyzing differences in signal intensities of peaks associated to the metabolites present in intact OPCs (see Table 2, Fig.1a). If we compared the proton spectra corresponding to P0, P15 and P60, for a given T_2-filter (TE), we could see that there were not large differences between ages (Fig.1b). However, at TE of 60 ms, a relative increase in most peak intensities at P15 is observed (Fig 1c-d). At long echo times (TE: 60 ms), the intensity of the peaks associated to macromolecules or molecules with low mobility decreases (i.e., molecules bound to membranes or intracellular structures). It is remarkable that one the most significant ($p < 0.05$) signal change corresponds to myo-inositol, a metabolite known to be present in cell cytoplasm. Signal intensities depend on their T_2 relaxation time, which is directly related to the molecular mobility in the cytoplasm. The higher metabolite mobility at P15 suggests a lower viscosity in the cytoplasm and low interaction between metabolites and the cytoskeleton, which as shown later, are associated with a decreased in the migratory capability and a decrease proliferation rate. These results indicate that OPCs isolated at P15 display intrinsic differences to those isolated at P0 or P60.

Since the differences in the metabolic patterns may give rise to differences in other aspects of OPC behaviour, such as proliferation and migration, it was not surprising that the rate of proliferation was significantly higher at P0 and lowest at P15 (Fig. 2a). Notably, OPCs isolated from adults (P60) proliferated at an intermediate rate (Fig. 2a) and in general, there was a significant decrease in the migratory capacities of OPCs with age (Fig. 2b). This was corroborated by video time-lapse analysis, where P15 (the slowest) and P60 OPCs migrated slower than perinatal OPCs (Fig. 2c). Moreover, P60

302 OPCs stopped least often during their migration (Table 2) and in total; P0 OPCs
303 migrated further while P15 OPCs migrated over the shortest distance (P0, 332μm; P15,
304 128μm; P60, 210 μm). These data highlight the heterogeneity in OPC behaviour (i.e.,
305 proliferation rate and migratory properties) under basal conditions, which could be
306 related to differences in their metabolic pattern and variation in relaxation times of
307 metabolites (i.e., cytoplasm viscosity). The strongest differences were detected in P15
308 OPCs, which may reflect the large scale myelination that is ongoing at that time [48,49].

309 **Migrating OPCs respond dynamically to FGF2 and anosmin-1 in an age-**
310 **dependent manner**

311 FGF-2 and anosmin-1 exert distinct chemotropic effects on rat SVZ neuroblasts, and on
312 rodent embryonic and postnatal OPCs, mainly acting via FGFR1 [19,27,32,33,40,50].
313 Hence, these molecules represent a good tool to systematically study the physiological
314 heterogeneity in OPC populations, avoiding the variability in structure and origin by
315 restricting our study to cerebral cortex OPCs. Exposure of OPCs isolated at different
316 stages (E16, P0, P7, P15 and P60) to FGF2 homogeneously increased the number of
317 transmigrating cells, confirming the previously described chemoattractive effect of this
318 factor (and its potential motogenic effect as well: Fig. 3a). The effect of FGF2 on
319 migration was significantly stronger on OPCs isolated from E16 and early postnatal
320 stages (P0 and P7) than on those from later stages, reflecting a gradual loss of
321 sensitivity with age and CNS maturation. Interestingly, anosmin-1 induced different
322 OPC responses depending on the age of the cells: neutral for E16 OPCs; significant
323 chemoattraction of OPCs isolated at P0 and P7; chemorepulsion in young adults (P15
324 and P60: Fig.3a). At all ages except P0, FGF2 triggered a stronger OPC response than
325 anosmin-1 (Fig. 3a).

326 To more clearly distinguish between the chemotropic and motogenic effects of FGF2
327 and anosmin-1 (direction or rate of migration), we followed OPCs from different aged
328 mice by video time-lapse microscopy. FGF2 increased the motility of OPCs at all the
329 stages studied and it increased the velocity of OPCs by around 20% relative to their
330 counterparts in control conditions (Fig. 3b). By contrast, anosmin-1 augmented the
331 motility of P0 OPCs, yet it clearly reduced the speed of P15 and P60 OPCs (Fig.3b).
332 Interestingly, P0 OPCs migrated further in the presence of either of the molecules tested
333 than in control conditions, and they stopped less frequently (Table 2). On the other

334 hand, P15 and P60 OPCs behaved similarly, migrating further and with fewer stops in
335 the presence of FGF2, and anosmin-1 exerted exactly the opposite effects (Fig. 3c-h;
336 Table 2). Together, our results suggest that both FGF2 and anosmin-1 mainly influence
337 the motility of OPCs (motogenic effects), consistent with previous data from our group
338 [19,27].

339 **Migration of human OPCs in the presence of FGF2 and anosmin-1**

340 As indicated above, molecules involved in the migration of OPCs during development
341 are up-regulated in the adult in conjunction with demyelination (including that
342 occurring in MS lesions in humans), suggesting the need to test the effects of these
343 molecules in adult OPCs. To complement this analysis, we sought to obtain information
344 from human adult OPCs, evaluating the effects of both anosmin-1 and FGF2on three
345 kinds of human OPCs in chemotaxis chambers: an oligodendroglioma cell line (HOG
346 cells), and on OPCs isolated from tumor tissueand non-tumor tissue obtained through
347 neurosurgery (the exact origin of these samples is indicated in the Methods). We first
348 confirmed that these three cell types expressed FGFR1, the receptor thought to mediate
349 the effects of FGF2 and anosmin-1 on OPC migration (Fig. 4a-f; [27,32,51-53]). It was
350 not surprising to find that the tumor-derived OPCs were more motile in control
351 conditions than non-tumoral OPCs (Table 3). However, exposure to the two factors
352 tested also produced differences, whereby the number of transmigrated non-tumor
353 OPCs significantly increased in the presence of FGF2 and was significantly lower in the
354 presence of anosmin-1(Fig. 4g, j-l), response similar to those of P60 mouse OPCs (Fig.
355 3a). In addition, both proteins were motogenic and acted as chemoattractants for tumor-
356 derived OPCs and HOG cells (Fig. 4h-l), as also reported for P0 murine OPCs (Fig. 3a).
357 It should be noted that the effect of anosmin-1 was stronger on OPCs isolated from
358 tumor samples than on the immortalized cell line. Video time-lapse analysis of non-
359 tumor isolated OPCs revealed that anosmin-1 reduced their migration velocity and the
360 distance they migrated, while increasing the number of stops, the opposite effect to that
361 observed with FGF2 for the same three parameters (Fig.5a-j, Table 3), reflecting the
362 contribution of pathological environment to the heterogeneity of OPC behaviour.
363 Together, these results from adult OPCs demonstrated that they are a heterogeneous
364 population of cells, in which the physiological heterogeneity depends on the species and
365 age. Indeed, this highlights the risk of directly extrapolating from drug testing on OPCs
366 isolated from neonatal/early postnatal rodent brains to the human adult scenario.

367 **The biological effects of FGF2 and anosmin-1 on OPC proliferation and**
368 **differentiation**

369 Rather than limiting our study to cell migration, we also studied how FGF2 and
370 anosmin-1 affected OPC proliferation and differentiation. Both these factors had a
371 constant effect on cell proliferation and while FGF2 significantly increased the number
372 of newly-generated OPCs at each developmental stage analyzed and in young mature
373 OPCs, anosmin-1 had no evident effect whatsoever on cell proliferation (Supplementary
374 Fig.1a). Regarding OPC differentiation towards myelin-forming phenotypes, more
375 heterogeneous results were obtained. In OPCs from embryonic (E16) and young adult
376 (P60) stages, neither of these factors altered the rate of differentiation relative to the
377 control conditions (Fig.6a-c, j-l, m). By contrast, FGF2 and anosmin-1 exerted opposite
378 effects on P0 cells, while both these factors drove P15 OPCs towards a myelinating
379 phenotype (Fig.6d-f, m).

380 **The effects of FGF2 and anosmin-1 on OPCs are FGFR-dependent**

381 FGF2 and its receptors have been implicated in numerous processes, including cell
382 proliferation, migration, differentiation and survival (for reviews see: [54-56]).
383 Although we previously demonstrated that FGF2 and anosmin-1 exert their effects on
384 OPC migration via FGFR1 [19,27,33,50,53], we analyzed the expression of the 3
385 FGFRs present in the oligodendroglial lineage [57,58] in our cultures of OPCs obtained
386 from mice of different ages (E16, P0, P15 and P60). The FGFR1 was expressed by
387 murine OPCs at every stage analyzed (Fig.7 a-l). Thus, to confirm that FGFR1
388 influences OPC migration, we repeated the chemotaxis assays on P0 (both anosmin-1
389 and FGF2 acting as chemoattractants) and P15 OPCs (anosmin-1 no effect; FGF2
390 chemoattractant), in the presence or absence of an FGFR signaling inhibitor (SU5402).
391 This inhibitor abrogated both the chemoattraction and chemorepulsion provoked by
392 FGF2 and/or anosmin-1, confirming FGFR1 as the FGF receptor involved in P0 and
393 P15 OPC migration (Fig. 7m).

394 In terms of OPC differentiation, SU5402 abolished the effects of both molecules at P0,
395 reducing the percentage of CNPase$^+$ cells to control levels, although it failed to achieve
396 the same effect on P15 OPCs exposed to either FGF2 or anosmin-1 (Fig.7n). As FGF2
397 binds to every FGFR but anosmin-1 binds exclusively to FGFR1 [52,53], it suggests
398 that other FGFRs expressed by OPCs at this stage are likely to be involved in their

399 differentiation [57-59]. Finally, when we analyzed the effect of SU5402 on OPC
400 proliferation, we noted that the increase in proliferation observed in the presence of
401 FGF2 was abolished with the inhibitor (Supplementary Fig. 1b).

402 Finally, we found a decrease in FGFR1 expression with age, which was most strongly
403 expressed at the embryonic stage analyzed (Fig. 7o). This gradual decline mirrors the
404 decrease in migration speed and chemotaxis in the presence of FGF2 and anosmin-
405 1with age (Fig. 1). In parallel, FGFR2 expression was weakest at P0, with no
406 remarkable changes at the other three stages studied (Fig. 7o). Finally, FGFR3
407 expression gradually increasing with age, from very weak expression at E16 to
408 approximately 1.5-fold stronger expression at P15 and P60 than at P0 (Fig. 7o),
409 consistent with previous reports [58].

410

411 **DISCUSSION**

412 Given their relative abundance in the adult CNS, their ability to move towards lesion
413 sites and their effectiveness in remyelination, there is ever increasing interest in adult
414 OPCs. However, this is a highly heterogeneous cell population and in practical terms,
415 the capacity of these cells to remyelinate lesions is limited [12,19,21,60-63]. Different
416 developmental signaling cues, including growth factors, are over expressed locally in
417 damaged areas, and they determine the survival, proliferation, migration and correct
418 differentiation of endogenous adult OPCs [18,19,23,24,64] (for a review see [65,66]).
419 Here we systematically studied heterochronic OPCs isolated from the mouse cerebral
420 cortex at E16, P0, P15 and P60, as well as OPCs isolated from samples of adult human
421 cerebral neocortex, avoiding the interference of the potential differences derived from
422 the different developmental origins of the cells [2].

423 The heterogeneity in the responses of the OPCs also varied in function of the factor to
424 which the cells were exposed. In response to FGF-2, OPCs responded in a more
425 consistent manner when proliferation and migration were explored than when
426 differentiation was studied. At each developmental stage studied, as well as in OPCs
427 isolated from the cerebral cortex of adult mice and humans, FGF2 significantly
428 enhanced cell proliferation (consistent with previous reports [55,67,68]) and certain
429 migratory parameters, reflecting a motogenic and chemoattractive effect as reported
430 previously [19,27,32,57,69]. It is interesting that the effect on human OPCs isolated
431 from the safety-margins of tumors was, in absolute numbers, stronger than that on
432 human adult OPCs isolated from non-tumor samples or even HOG cells (of human
433 origin). It is also true that P15 OPCs had both a lower rate of proliferation and poorer
434 mobility than the OPCs isolated from P0 and P60 mice. Our data on OPC differentiation
435 towards myelin-forming phenotypes substantially differed with age. As such, while
436 FGF2 interfered with OPC differentiation of P0 OPCs (as indicated elsewhere [59,70]),
437 it favored the differentiation of P15 OPCs and it had a neutral effect on OPCs isolated
438 from the adult cerebral cortex, independent of the species (similar results were obtained
439 with rat P0 OPCs –data not shown- and adult human OPCs). NMR on murine OPCs
440 also identified different metabolic patterns, and the less viscous cytoplasm of P15 OPCs
441 compared to that of those isolated at P0 or P60 could explain the decreased in the
442 migratory activity and proliferation OPCs at these stages [71-73]. This novel technique

443 was previously used to analyze extracts of different cells types, including stem cells
444 [74,75], although it was not applied to intact cells as occurred here.

445 In contrast to FGF2, anosmin-1 had no effect on OPC proliferation and it only
446 potentiated OPC differentiation at early stages (P0, P15), having a neutral effect on
447 differentiation at adult stages. However, the effects of anosmin-1 on OPC migration
448 differed dramatically in function of both species and age, increasing the motility of P0
449 and tumor-related human OPCs (cells isolated from the safety-margins of tumors and
450 also the HOG cell line), while it slowed down the migration of P15 and P60/adult
451 OPCs, and that of OPCs from human non-tumor samples. These latter experiments
452 confirmed earlier data and to some extent they explain the factors that condition OPC
453 responses to anosmin-1 [27,32,33].

454 With respect to the different effects observed with human OPCs and other tumor cells,
455 anosmin-1 seems to promote/attract the migration of tumor cells and immortalized cell
456 lines ([52,76-79]; data herein). This might contribute to cancer cell dispersion and
457 metastasis, while anosmin-1 can contribute to the immobilization of cells in both
458 physiological conditions (data herein) and in non-tumoral diseases like MS [19].
459 Nevertheless, it was suggested elsewhere that the*Kal-1* gene would be a suppressor for
460 other cancer types [78,80], which merits more systematic study. Likewise, the opposing
461 or cooperative effects of FGF2 and anosmin-1 on tumor cells are still to be evaluated.

462 Undoubtedly, our study provides particularly interesting results in terms of the
463 similarities and differences between OPCs isolated from the murine and human adult
464 brain. The migratory properties of adult OPCs isolated from both species displayed
465 parallel responses to FGF2 and anosmin-1, which is far from similar to the responses
466 observed in early postnatal OPCs. Thus, our data demonstrate that OPC heterogeneity
467 depends not only on the anatomical region from where they are isolated and on the way
468 they respond to injury [21,81] but also, on the species, the stage in the life cycle and the
469 functional system to which they pertain. This phenomenon should be taken into account
470 in future studies that search for pharmacological agents to promote the motility of
471 human OPCs isolated from different origins (the fetal or adult brain) in order to drive
472 remyelination [66,82,83]. As such, and irrespective of their origin (murine or human),
473 adult OPCs behave distinctly to OPCs isolated at earlier stages at least in part because
474 their metabolic profiles are very different. In addition, their response to different cues,

475 such as FGF2 and anosmin-1, is modified with age. Although not as systematic as our
476 current work, earlier data also suggest that the effects triggered by growth factors and
477 motogenic cues (PDGF, FGF2) are more constant than those driven by chemotropic
478 molecules and/or cytokines (semaphorins, netrin, anosmin-1, CCLs [35,65,84,85].
479 Hence, these data together probably reflect a hierarchy among the different molecules
480 that influence the biology of OPCs during development and in different species.

481 In conclusion, the data presented here help understand the response of endogenous
482 OPCs to lesion in the adult CNS. As such, therapeutic approaches for neurodegenerative
483 diseases should focus on the potentiation of the endogenous OPCs present in the adult
484 brain, enhancing their spontaneous remyelinating capacity. Accordingly, it should also
485 be borne in mind that the modulation of FGF family members might also improve
486 myelin repair in diseases like MS.

487

REFERENCES

[1] Dawson MR, Polito A, Levine JM, Reynolds R (2003) NG2-expressing glial progenitor cells: an abundant and widespread population of cycling cells in the adult rat CNS. Mol Cell Neurosci 24: 476-488. doi: 10.1016/S1044-7431(03)00210-0

[2] de Castro F, Zalc B (2013) Migration of Myelin-Forming Cells in the CNS. In: Rubenstein JLR, Rakic P, editors. Comprehensive Developmental Neuroscience: Cellular Migration and Formation of Neuronal Connections. Elsevier, Amsterdam, p 417-429.

[3] McKenzie IA, Ohayon D, Li H, de Faria JP, Emery B, Tohyama K, Richardson WD (2014) Motor skill learning requires active central myelination. Science 346: 318-322. doi: 10.1126/science.1254960

[4] Richardson WD, Kessaris N, Pringle N (2006) Oligodendrocyte wars. Nat Rev Neurosci 7: 11-18. doi: 10.1038/nrn1826

[5] Young KM, Psachoulia K, Tripathi RB, Dunn SJ, Cossell L, Attwell D, Tohyama K, Richardson WD (2013) Oligodendrocyte dynamics in the healthy adult CNS: evidence for myelin remodeling. Neuron 77: 873-885. doi: 10.1016/j.neuron.2013.01.006

[6] Dimou L, Simon C, Kirchhoff F, Takebayashi H, Gotz M (2008) Progeny of Olig2-expressing progenitors in the gray and white matter of the adult mouse cerebral cortex. J Neurosci 28: 10434-10442. doi: 10.1523/JNEUROSCI.2831-08.2008

[7] Dimou L, Gallo V (2015) NG2-glia and their functions in the central nervous system. Glia 63: 1429-1451. doi: 10.1002/glia.22859

[8] Kang SH, Fukaya M, Yang JK, Rothstein JD, Bergles DE (2010) NG2+ CNS glial progenitors remain committed to the oligodendrocyte lineage in postnatal life and following neurodegeneration. Neuron 68: 668-681. doi: 10.1016/j.neuron.2010.09.009

[9] Psachoulia K, Jamen F, Young KM, Richardson WD (2009) Cell cycle dynamics of NG2 cells in the postnatal and ageing brain. Neuron Glia Biol 5: 57-67. doi: 10.1017/S1740925X09990354

[10] Rivers LE, Young KM, Rizzi M, Jamen F, Psachoulia K, Wade A, Kessaris N, Richardson WD (2008) PDGFRA/NG2 glia generate myelinating oligodendrocytes and piriform projection neurons in adult mice. Nat Neurosci 11: 1392-1401. doi: 10.1038/nn.2220

[11] Zhu Q, Whittemore SR, Devries WH, Zhao X, Kuypers NJ, Qiu M (2011) Dorsally-derived oligodendrocytes in the spinal cord contribute to axonal myelination during development and remyelination following focal demyelination. Glia 59: 1612-1621. doi: 10.1002/glia.21203

527 [12] Hill RA, Nishiyama A (2014) NG2 cells (polydendrocytes): listeners to the
528 neural network with diverse properties. Glia 62: 1195-1210. doi:
529 10.1002/glia.22664

530 [13] Richardson WD, Young KM, Tripathi RB, McKenzie I (2011) NG2-glia as
531 multipotent neural stem cells: fact or fantasy? Neuron 70: 661-673. doi:
532 10.1016/j.neuron.2011.05.013

533 [14] Calver AR, Hall AC, Yu WP, Walsh FS, Heath JK, Betsholtz C, Richardson
534 WD (1998) Oligodendrocyte population dynamics and the role of PDGF in vivo.
535 Neuron 20: 869-882. doi: 10.1016/S0896-6273(00)80469-9

536 [15] Simon C, Gotz M, Dimou L (2011) Progenitors in the adult cerebral cortex: cell
537 cycle properties and regulation by physiological stimuli and injury. Glia 59:
538 869-881. doi: 10.1002/glia.21156

539 [16] Nishiyama A, Komitova M, Suzuki R, Zhu X (2009) Polydendrocytes (NG2
540 cells): multifunctional cells with lineage plasticity. Nat Rev Neurosci 10: 9-22.
541 doi: 10.1038/nrn2495

542 [17] Seo JH, Miyamoto N, Hayakawa K, Pham LD, Maki T, Ayata C, Kim KW, Lo
543 EH, Arai K (2013) Oligodendrocyte precursors induce early blood-brain barrier
544 opening after white matter injury. J Clin Invest 123: 782-786. doi:
545 10.1172/JCI65863

546 [18] Boyd A, Zhang H, Williams A (2013) Insufficient OPC migration into
547 demyelinated lesions is a cause of poor remyelination in MS and mouse models.
548 Acta Neuropathol 125: 841-859. doi: 10.1007/s00401-013-1112-y

549 [19] Clemente D, Ortega MC, Arenzana FJ, de Castro F (2011) FGF-2 and Anosmin-
550 1 are selectively expressed in different types of multiple sclerosis lesions. J
551 Neurosci 31: 14899-14909. doi: 10.1523/JNEUROSCI.1158-11.2011

552 [20] Ferent J, Zimmer C, Durbec P, Ruat M, Traiffort E (2013) Sonic Hedgehog
553 signaling is a positive oligodendrocyte regulator during demyelination. J
554 Neurosci 33: 1759-1772. doi: 10.1523/JNEUROSCI.3334-12.2013

555 [21] Moyon S, Dubessy AL, Aigrot MS, Trotter M, Huang JK, Dauphinot L, Potier
556 MC, Kerninon C, Melik PS, Franklin RJ, Lubetzki C (2015) Demyelination
557 causes adult CNS progenitors to revert to an immature state and express immune
558 cues that support their migration. J Neurosci 35: 4-20. doi:
559 10.1523/JNEUROSCI.0849-14.2015

560 [22] Ortega JA, Radonjic NV, Zecevic N (2013) Sonic hedgehog promotes
561 generation and maintenance of human forebrain Olig2 progenitors. Front Cell
562 Neurosci 7: 254. doi: 10.3389/fncel.2013.00254

563 [23] Piaton G, Williams A, Seilhean D, Lubetzki C (2009) Remyelination in multiple
564 sclerosis. Prog Brain Res 175: 453-464. doi: 10.1016/S0079-6123(09)17530-1

565 [24] Williams A, Piaton G, Aigrot MS, Belhadi A, Theaudin M, Petermann F,
566 Thomas JL, Zalc B, Lubetzki C (2007) Semaphorin 3A and 3F: key players in

567 myelin repair in multiple sclerosis? Brain 130: 2554-2565. doi:
568 10.1093/brain/awm202

569 [25] Díaz-Balzac CA, Lázaro-Pena MI, Ramos-Ortiz GA, Bulow HE (2015) The
570 Adhesion Molecule KAL-1/anosmin-1 Regulates Neurite Branching through a
571 SAX-7/L1CAM-EGL-15/FGFR Receptor Complex. Cell Rep 11: 1377-1384.
572 doi: 10.1016/j.celrep.2015.04.057

573 [26] Azin M, Mirnajafi-Zadeh J, Javan M (2015) Fibroblast Growth Factor-2
574 Enhanced The Recruitment of Progenitor Cells and Myelin Repair in
575 Experimental Demyelination of Rat Hippocampal Formations. Cell J 17: 540-
576 456.

577 [27] Bribián A, Barallobre MJ, Soussi-Yanicostas N, de Castro F (2006) Anosmin-1
578 modulates the FGF-2-dependent migration of oligodendrocyte precursors in the
579 developing optic nerve. Mol Cell Neurosci 33: 2-14. doi:
580 10.1016/j.mcn.2006.05.009

581 [28] Bribián A, Esteban PF, Clemente D, Soussi-Yanicostas N, Thomas JL, Zalc B,
582 de Castro F (2008) A novel role for anosmin-1 in the adhesion and migration of
583 oligodendrocyte precursors. Dev Neurobiol 68: 1503-1516. doi:
584 10.1002/dneu.20678

585 [29] Endo Y, Ishiwata-Endo H, Yamada KM (2012) Extracellular matrix protein
586 anosmin promotes neural crest formation and regulates FGF, BMP, and WNT
587 activities. Dev Cell 23: 305-316. doi: 10.1016/j.devcel.2012.07.006

588 [30] Hu Y, Poopalasundaram S, Graham A, Bouloux PM (2013) GnRH neuronal
589 migration and olfactory bulb neurite outgrowth are dependent on FGF receptor 1
590 signaling, specifically via the PI3K p110alpha isoform in chick embryo.
591 Endocrinology 154: 388-399. doi: 10.1210/en.2012-1555

592 [31] Mierzwa AJ, Zhou YX, Hibbits N, Vana AC, Armstrong RC (2013) FGF2 and
593 FGFR1 signaling regulate functional recovery following cuprizone
594 demyelination. Neurosci Lett 548: 280-285. doi: 10.1016/j.neulet.2013.05.010

595 [32] Murcia-Belmonte V, Medina-Rodríguez EM, Bribián A, de Castro F, Esteban
596 PF (2014) ERK1/2 signaling is essential for the chemoattraction exerted by
597 human FGF2 and human anosmin-1 on newborn rat and mouse OPCs via
598 FGFR1. Glia 62: 374-386. doi: 10.1002/glia.22609

599 [33] Murcia-Belmonte V, Esteban PF, Martínez-Hernández J, Gruart A, Lujan R,
600 Delgado-Garcia JM, de Castro F (2016) Anosmin-1 over-expression regulates
601 oligodendrocyte precursor cell proliferation, migration and myelin sheath
602 thickness. Brain Struct Funct 221: 1365-1385. doi: 10.1007/s00429-014-0977-4

603 [34] Medina-Rodríguez EM, Arenzana FJ, Bribián A, de Castro F (2013) Protocol to
604 isolate a large amount of functional oligodendrocyte precursor cells from the
605 cerebral cortex of adult mice and humans. PLoS One 8: e81620. doi:
606 10.1371/journal.pone.0081620

607 [35] Bin JM, Rajasekharan S, Kuhlmann T, Hanes I, Marcal N, Han D, Rodrigues
608 SP, Leong SY, Newcombe J, Antel JP, Kennedy TE (2013) Full-length and
609 fragmented netrin-1 in multiple sclerosis plaques are inhibitors of
610 oligodendrocyte precursor cell migration. Am J Pathol 183: 673-680. doi:
611 10.1016/j.ajpath.2013.06.004

612 [36] Cui QL, Kuhlmann T, Miron VE, Leong SY, Fang J, Gris P, Kennedy TE,
613 Almazan G, Antel J (2013) Oligodendrocyte progenitor cell susceptibility to
614 injury in multiple sclerosis. Am J Pathol 183: 516-525. doi:
615 10.1016/j.ajpath.2013.04.016

616 [37] John GR (2012) Investigation of astrocyte - oligodendrocyte interactions in
617 human cultures. Methods Mol Biol 814: 401-414. doi: 10.1007/978-1-61779-
618 452-0_27

619 [38] Medina-Rodríguez EM, Arenzana FJ, Pastor J, Redondo M, Palomo V, García
620 de Sola R, Gil C, Martínez A, Bribián A, de Castro F (2013) Inhibition of
621 endogenous phosphodiesterase 7 promotes oligodendrocyte precursor
622 differentiation and survival. Cell Mol Life Sci 70: 3449-3462. doi:
623 10.1007/s00018-013-1340-2

624 [39] Soussi-Yanicostas N, Hardelin JP, Arroyo-Jiménez MM, Ardouin O, Legouis R,
625 Levilliers J, Traincard F, Betton JM, Cabanie L, Petit C (1996) Initial
626 characterization of anosmin-1, a putative extracellular matrix protein
627 synthesized by definite neuronal cell populations in the central nervous system. J
628 Cell Sci 109 (Pt 7): 1749-1757.

629 [40] García-González D, Clemente D, Coelho M, Esteban PF, Soussi-Yanicostas N,
630 de Castro F (2010) Dynamic roles of FGF-2 and Anosmin-1 in the migration of
631 neuronal precursors from the subventricular zone during pre- and postnatal
632 development. Exp Neurol 222: 285-295. doi: 10.1016/j.expneurol.2010.01.006

633 [41] Casaccia-Bonnefil P, Tikoo R, Kiyokawa H, Friedrich V, Jr., Chao MV, Koff A
634 (1997) Oligodendrocyte precursor differentiation is perturbed in the absence of
635 the cyclin-dependent kinase inhibitor p27Kip1. Genes Dev 11: 2335-2346. doi:
636 10.1101/gad.11.18.2335

637 [42] Rocha CM, Barros AS, Gil AM, Goodfellow BJ, Humpfer E, Spraul M, Carreira
638 IM, Melo JB, Bernardo J, Gomes A, Sousa V, Carvalho L, Duarte IF (2010)
639 Metabolic profiling of human lung cancer tissue by 1H high resolution magic
640 angle spinning (HRMAS) NMR spectroscopy. J Proteome Res 9: 319-332. doi:
641 10.1021/pr9006574

642 [43] Moestue S, Sitter B, Bathen TF, Tessem MB, Gribbestad IS (2011) HR MAS
643 MR spectroscopy in metabolic characterization of cancer. Curr Top Med Chem
644 11: 2-26. doi: 10.2174/156802611793611869

645 [44] Govindaraju V, Young K, Maudsley AA (2000) Proton NMR chemical shifts
646 and coupling constants for brain metabolites. NMR Biomed 13: 129-153.

647 [45] Cheng LL, Lean CL, Bogdanova A, Wright SC, Jr., Ackerman JL, Brady TJ,
648 Garrido L (1996) Enhanced resolution of proton NMR spectra of malignant

649 lymph nodes using magic-angle spinning. Magn Reson Med 36: 653-658. doi:
650 10.1002/mrm.1910360502

651 [46] Griffin JL, Bollard M, Nicholson JK, Bhakoo K (2002) Spectral profiles of
652 cultured neuronal and glial cells derived from HRMAS (1)H NMR
653 spectroscopy. NMR Biomed 15: 375-384. doi: 10.1002/nbm.792

654 [47] Lindon JC, Beckonert OP, Holmes E, Nicholson JC (2009) High resolution
655 magic angle spinning NMR spectroscopy: Application to biomedical studies.
656 Prog. NMR Spectrosc 55: 79-100. doi: 10.1016/j.pnmrs.2008.11.004

657 [48] Flores AI, Narayanan SP, Morse EN, Shick HE, Yin X, Kidd G, Avila RL,
658 Kirschner DA, Macklin WB (2008) Constitutively active Akt induces enhanced
659 myelination in the CNS. J Neurosci 28: 7174-7183. doi:
660 10.1523/JNEUROSCI.0150-08.2008

661 [49] Lu Z, Ku L, Chen Y, Feng Y (2005) Developmental abnormalities of myelin
662 basic protein expression in fyn knock-out brain reveal a role of Fyn in
663 posttranscriptional regulation. J Biol Chem 280: 389-395. doi:
664 10.1074/jbc.M405973200

665 [50] Esteban PF, Murcia-Belmonte V, García-González D, de Castro F (2013) The
666 cysteine-rich region and the whey acidic protein domain are essential for
667 anosmin-1 biological functions. J Neurochem 124: 708-720. doi:
668 10.1111/jnc.12104

669 [51] González-Martínez D, Kim SH, Hu Y, Guimond S, Schofield J, Winyard P,
670 Vannelli GB, Turnbull J, Bouloux PM (2004) Anosmin-1 modulates fibroblast
671 growth factor receptor 1 signaling in human gonadotropin-releasing hormone
672 olfactory neuroblasts through a heparan sulfate-dependent mechanism. J
673 Neurosci 24: 10384-10392. doi: 10.1523/JNEUROSCI.3400-04.2004

674 [52] Hu Y, Guimond SE, Travers P, Cadman S, Hohenester E, Turnbull JE, Kim SH,
675 Bouloux PM (2009) Novel mechanisms of fibroblast growth factor receptor 1
676 regulation by extracellular matrix protein anosmin-1. J Biol Chem 2009; 284:
677 29905-29920. doi: 10.1074/jbc.M109.049155

678 [53] Murcia-Belmonte V, Esteban PF, García-González D, de Castro F (2010)
679 Biochemical dissection of Anosmin-1 interaction with FGFR1 and components
680 of the extracellular matrix. J Neurochem 115: 1256-1265. doi: 10.1111/j.1471-
681 4159.2010.07024.x

682 [54] Bansal R, Pfeiffer SE (1997) FGF-2 converts mature oligodendrocytes to a
683 novel phenotype. J Neurosci Res 50: 215-228. doi: 10.1002/(SICI)1097-
684 4547(19971015)50:2%3C215::AID-JNR10%3E3.3.CO;2-8

685 [55] Bansal R (2002) Fibroblast growth factors and their receptors in oligodendrocyte
686 development: implications for demyelination and remyelination. Dev Neurosci
687 24: 35-46. doi: 10.1159/000064944

688 [56] Oh LY, Yong VW (1996) Astrocytes promote process outgrowth by adult
689 human oligodendrocytes in vitro through interaction between bFGF and

690 astrocyte extracellular matrix. Glia 17: 237-253. doi: 10.1002/(SICI)1098-
691 1136(199607)17:3%3C237::AID-GLIA6%3E3.0.CO;2-Y

692 [57] Bansal R, Kumar M, Murray K, Morrison RS, Pfeiffer SE (1996) Regulation of
693 FGF receptors in the oligodendrocyte lineage. Mol Cell Neurosci 7: 263-275.
694 doi: 10.1006/mcne.1996.0020

695 [58] Fortin D, Rom E, Sun H, Yayon A, Bansal R (2005) Distinct fibroblast growth
696 factor (FGF)/FGF receptor signaling pairs initiate diverse cellular responses in
697 the oligodendrocyte lineage. J Neurosci 25: 7470-7479. doi:
698 10.1523/JNEUROSCI.2120-05.2005

699 [59] Furusho M, Dupree JL, Nave KA, Bansal R (2012) Fibroblast growth factor
700 receptor signaling in oligodendrocytes regulates myelin sheath thickness. J
701 Neurosci 2012; 32: 6631-6641. doi: 10.1523/JNEUROSCI.6005-11.2012

702 [60] Franklin RJ, Gallo V (2014) The translational biology of remyelination: past,
703 present, and future. Glia 2014; 62: 1905-1915. doi: 10.1002/glia.22622

704 [61] Maki T, Liang AC, Miyamoto N, Lo EH, Arai K (2013) Mechanisms of
705 oligodendrocyte regeneration from ventricular-subventricular zone-derived
706 progenitor cells in white matter diseases. Front Cell Neurosci 7: 275. doi:
707 10.3389/fncel.2013.00275

708 [62] Nishiyama A (2007) Polydendrocytes: NG2 cells with many roles in
709 development and repair of the CNS. Neuroscientist 13: 62-76. doi:
710 10.1177/1073858406295586

711 [63] Tepavcevic DK, Pekmezovic T, Stojsavljevic N, Kostic J, Basuroski ID,
712 Mesaros S, Drulovic J (2014) Change in quality of life and predictors of change
713 among patients with multiple sclerosis: a prospective cohort study. Qual Life
714 Res 23: 1027-1037. doi: 10.1007/s11136-013-0535-1

715 [64] Syed YA, Baer A, Hofer MP, González GA, Rundle J, Myrta S, Huang JK, Zhao
716 C, Rossner MJ, Trotter MW, Lubec G, Franklin RJ, Kotter MR (2013) Inhibition
717 of phosphodiesterase-4 promotes oligodendrocyte precursor cell differentiation
718 and enhances CNS remyelination. EMBO Mol Med 5:1918-1934. doi:
719 10.1002/emmm.201303123

720 [65] de Castro F, Bribián A, Ortega MC (2013) Regulation of oligodendrocyte
721 precursor migration during development, in adulthood and in pathology. Cell
722 Mol Life Sci 70: 4355-4368. doi: 10.1007/s00018-013-1365-6

723 [66] Huang JK, Franklin RJ (2011) Regenerative medicine in multiple sclerosis:
724 identifying pharmacological targets of adult neural stem cell differentiation.
725 Neurochem Int 59: 329-332. doi: 10.1016/j.neuint.2011.01.017

726 [67] Azim K, Raineteau O, Butt AM (2012) Intraventricular injection of FGF-2
727 promotes generation of oligodendrocyte-lineage cells in the postnatal and adult
728 forebrain. Glia 60: 1977-1990. doi: 10.1002/glia.22413

729 [68] Murtie JC, Zhou YX, Le TQ, Vana AC, Armstrong RC (2005) PDGF and FGF2
730 pathways regulate distinct oligodendrocyte lineage responses in experimental
731 demyelination with spontaneous remyelination. Neurobiol Dis 19: 171-182. doi:
732 10.1016/j.nbd.2004.12.006

733 [69] McKinnon RD, Smith C, Behar T, Smith T, Dubois-Dalcq M (1993) Distinct
734 effects of bFGF and PDGF on oligodendrocyte progenitor cells. Glia 7: 245-254.
735 doi: 10.1002/glia.440070308

736 [70] Furusho M, Roulois AJ, Franklin RJ, Bansal R (2015) Fibroblast growth factor
737 signaling in oligodendrocyte-lineage cells facilitates recovery of chronically
738 demyelinated lesions but is redundant in acute lesions. Glia 63: 1714-1728. doi:
739 10.1002/glia.22838

740 [71] Lee K, Fodor WL, Machaty Z. 2007. Dynamics of lamin A/C in porcine
741 embryos produced by nuclear transfer. MolReprod Dev. 74:1221-1227. doi:
742 10.1002/mrd.20681

743 [72] Maniotis AJ, Chen CS, Ingber DE (1997) Demonstration of mechanical
744 connections between integrins, cytoskeletal filaments, and nucleoplasm that
745 stabilize nuclear structure.Proc Natl AcadSci U S A. 94:849-854. doi:
746 10.1073/pnas.94.3.849

747 [73] Pollard TD, Borisy GG (2003) Cellular motility driven by assembly and
748 disassembly of actin filaments. Cell 112: 453-465. doi: 10.1016/S0092-
749 8674(03)00120-X

750 [74] Jansen JF, Shamblott MJ, van Zijl PC, Lehtimäki KK, Bulte JW, Gearhart JD,
751 Hakumäki JM (2006) Stem cell profiling by nuclear magnetic resonance
752 spectroscopy.MagnReson Med. 56:666-670. doi: 10.1002/mrm.20968

753 [75] Urenjak J, Williams SR, Gadian DG, Noble M (1993) Proton nuclear magnetic
754 resonance spectroscopy unambiguously identifies different neural cell types. J
755 Neurosci 13: 981-989.

756 [76] Cariboni A, Pimpinelli F, Colamarino S, Zaninetti R, Piccolella M, Rumio C,
757 Piva F, Rugarli EI, Maggi R (2004) The product of X-linked Kallmann's
758 syndrome gene (KAL1) affects the migratory activity of gonadotropin-releasing
759 hormone (GnRH)-producing neurons. Hum Mol Genet 13: 2781-2791. doi:
760 10.1093/hmg/ddh309

761 [77] Choy CT, Kim H, Lee JY, Williams DM, Palethorpe D, Fellows G, Wright AJ,
762 Laing K, Bridges LR, Howe FA, Kim SH (2014) Anosmin-1 contributes to brain
763 tumor malignancy through integrin signal pathways. Endocr Relat Cancer 21:
764 85-99. doi: 10.1530/ERC-13-0181

765 [78] Jian B, Nagineni CN, Meleth S, Grizzle W, Bland K, Chaudry I, Raju R (2009)
766 Anosmin-1 involved in neuronal cell migration is hypoxia inducible and cancer
767 regulated. Cell Cycle 8: 3770-3776. doi: 10.4161/cc.8.22.10066

768 [79] Kanda M, Shimizu D, Fujii T, Sueoka S, Tanaka Y, Ezaka K, Takami H, Tanaka
769 H, Hashimoto R, Iwata N, Kobayashi D, Tanaka C, Yamada S, Nakayama G,

770 Sugimoto H, Koike M, Fujiwara M, Kodera Y (2016) Function and diagnostic
771 value of Anosmin-1 in gastric cancer progression. Int J Cancer 138: 721-730.
772 doi: 10.1002/ijc.29803

773 [80] Liu J, Cao W, Chen W, Xu L, Zhang C (2015) Decreased expression of
774 Kallmann syndrome 1 sequence gene (KAL1) contributes to oral squamous cell
775 carcinoma progression and significantly correlates with poorly differentiated
776 grade. J Oral Pathol Med 44: 109-114. doi: 10.1111/jop.12206

777 [81] Nishiyama A, Suzuki R, Zhu X (2014) NG2 cells (polydendrocytes) in brain
778 physiology and repair. Front Neurosci 8: 133. doi: 10.3389/fnins.2014.00133

779 [82] Dubois-Dalcq M, Ffrench-Constant C, Franklin RJ (2005) Enhancing central
780 nervous system remyelination in multiple sclerosis. Neuron 48: 9-12. doi:
781 10.1016/j.neuron.2005.09.004

782 [83] Leong SY, Rao VT, Bin JM, Gris P, Sangaralingam M, Kennedy TE, Antel JP
783 (2014) Heterogeneity of oligodendrocyte progenitor cells in adult human brain.
784 Ann Clin Transl Neurol 1: 272-283. doi: 10.1002/acn3.55

785 [84] Mitew S, Hay CM, Peckham H, Xiao J, Koenning M, Emery B (2014)
786 Mechanisms regulating the development of oligodendrocytes and central
787 nervous system myelin. Neuroscience 276: 29-47. doi:
788 10.1016/j.neuroscience.2013.11.029

789 [85] Tepavcevic V, Kerninon C, Aigrot MS, Meppiel E, Mozafari S, rnould-Laurent
790 R, Ravassard P, Kennedy TE, Nait-Oumesmar B, Lubetzki C (2014) Early
791 netrin-1 expression impairs central nervous system remyelination. Ann Neurol
792 76: 252-268. doi: 10.1002/ana.24201
793

AKNOWLEDGEMENTS

We thank Miss Iris Sánchez and Mr Rafael Lebrón for their technical support, as well as Dr José Ángel Rodríguez-Alfaro and Dr Javier Mazarío for their help with the imaging. This work was supported by grants from the Spanish Ministerio de Economía y Competitividad (MINECO: grant numbers SAF2009–07842, SAF2012-40023, RD07-0060-2007; and the Red Española de Esclerosis Múltiple: RD12-0032-12) and the ‘‘Fundación Eugenio Rodríguez Pascual’’ to FdC. ABA was hired under MINECO grants ADE10-0010 andSAF2012-40023. EMMR is the recipient of a predoctoral fellowship from the MINECO FPI program (BES-2010-042593 associated to SAF2009–07842). IM is contracted by SESCAM. FdC is a CSIC Staff Scientist.

Conflict of interest

Authors declare that there are no financial or conflicts of interests exist.

819 **FIGURE LEGENDS**

820 **Figure 1:** NMR of intact OPCs. Proton HR-MAS NMR spectra with water suppression
821 corresponding to a sample of OPCs (P15) illustrating the chemical shift assignment of
822 selected metabolites with T_2-filters of 2 ms (a) and 60 ms (c), and the intensities of the
823 metabolites indicated normalized with respect to creatine for T_2-filters of 2 ms (b) and
824 60 ms (d). An increase in the relative intensities of P15 metabolites with respect to those
825 of P0 and P60, for the T2-filter of 60 ms, is observed suggesting a decrease in
826 cytoplasm viscosity.

827 **Figure 2: OPC proliferation and migration rates differ with age.** a) Proliferation
828 rate of neonatal, postnatal and adult OPCs. The number of proliferating OPCs also
829 decreases with age. b) Transmigrated cells of different ages after 20 hours in control
830 conditions: E16, P0, P15 and P60. The number of transmigrated cells decreases with
831 age. c) Histogram represents the migration speed at P0, P15 and P60. The migration
832 speed is higher at P0, and it diminishes in OPCs from P15 and P60 mice. For all
833 experimental groups, the results were analyzed using ANOVA and a Student´s*t*-test:
834 *P<0.05, **P<0.01, and ***P<0.001.

835 **Figure 3: FGF2 and anosmin-1 control OPC migration**. a) Histograms showing the
836 proportion of OPCs relative to the controls quantified in the presence or absence of
837 FGF2 or anosmin-1 at different stages: E16, P0, P7, P15 and P60. ANOVA showed
838 anosmin-1 had no effect on migration at E16 and P7, in contrast to other stages, while
839 and effect of FGF2 was evident at all stages. b) Histogram from the video time lapse
840 analysis representing the speed of migration at P0, P15 and P60 in the presence of either
841 factor. c-e) Images show the manual tracking at the end of the video time lapse
842 recording for P0 OPCs, in control conditions (c) and in the presence of anosmin-1 (d) or
843 FGF-2 (e). f-h) Analysis of the total distance migrated after 18hoursin all conditions: P0
844 (f), P15 (g) and P60 (h).All experimental groups were analyzed with a Student´s *t*-test:
845 *P<0.05, **P<0.01, and ***P<0.001.

846 **Figure 4: Effect of FGF2 and anosmin-1 on human OPC migration**. Adult human
847 OPCs (a-c) and HOG cells (d-f) expressed FGFR1. In both types of tumor cell analyzed,
848 tumor cells (g) and HOG cells (h), the response to FGF2 and anosmin-1 was the same.
849 Non-tumor cells responded to FGF2 like tumor cells, while the response to anosmn-1 is
850 the opposite in these cell types (i). j-l) Images of tumor OPCs in chemotaxis chambers

851 stained with A2B5 (red). Scale bar represents 7.5µm for a-f and 25 µm for j-l. The
852 results were analyzed with a Student´s *t*-test: *P<0.05, **P<0.01, and ***P<0.001.

853 **Figure 5: Video time lapse imaging of human OPC migration**.(a-f) The manual
854 tracking of non-tumor human OPCs (a-c) and tumor OPCs (d-f). Non-tumor cells
855 migrate faster and further in the presence of FGF2 (g, i), while anosmin-1 has the
856 opposite effect. Anosmin-1 and FGF2 both induce faster (j) and further migration (k) of
857 tumor OPCs. The results were analyzed with a Student´s *t*-test: *P<0.05, **P<0.01, and
858 ***P<0.001.

859 **Figure 6: The effects of FGF2 and anosmin-1 on OPC differentiation**. Images show
860 mature oligodendrocytes from E16 (a-c), P0 (d-f), P15 (g-i) and P60 (j-l) mice labeled
861 with CNPase (green) in control conditions and in the presence of FGF2 or anosmin-1.
862 m) Histogram represents the proportion of $CNPase^+$ cells relative to the controls at all
863 the stages analyzed. Scale bar represents 25 µm for a-l and the results were analyzed
864 with a Student´s *t*-test: *P<0.05, **P<0.01, and ***P<0.001.

865 **Figure 7: FGFR expression and its influence on OPCs.** a-l) FGFR1 is expressed by
866 OPCs at all the stages analyzed: E16 (a-c), P0 (d-f), P15 (g-i) and P60 (j-l). m)
867 Histogram showing the results of chemotaxis at P0 and P15 in the presence of SU5402,
868 which reverts the effects of anosmin-1 and FGF2. n) $CNPase^+$ cells at P0 and P15 in
869 cultures treated with SU5402 or the vehicle alone. No changes were observed in the
870 presence of SU5402. o) FGFR1, R2 and R3 expression by OPCs isolated at E16, P0,
871 P15 and P60. Scale bar represents 7.5µm for a-c, g-i, and 10 µm for d-f, j-l. The results
872 were analyzed with a Student´s *t*-test: *P<0.05, **P<0.01, and ***P<0.001.

873

Table 1: Summary of human samples used for in vitro experiments

Patient	Age (years)/sex	Diagnostic	Lobe	Sample weight (gr)
540	51/Female	Epilepsy	Temporal	4,9
573	24/Male	Epilepsy	Temporal	2,9
T-590	47/Female	Tumoral	Temporal	1,9
554	50/Female	Epilepsy	Temporal	2,6
574	45/Female	Epilepsy	Temporal	1,4
559	45/Female	Epilepsy	Temporal	1,1
579	50/Male	Epilepsy	Temporal	2,6
603	53/Female	Epilepsy	Temporal	1,1
549	32/Female	Epilepsy	Temporal	2
641	27/Female	Epilepsy	Temporal	1,3
T-604	37/Female	Tumoral	Temporal	0,7
363	51/Female	Epilepsy	Temporal	4
583	40/Male	Epilepsy	Temporal	0,8
T-1-SC	62/Female	Tumoral	Temporal	0,2
T-2-SC	68/Male	Tumoral	Temporal	0,6
T-3-SC	61/Female	Tumoral	Temporal	1,5
T-5-SC	51/Female	Tumoral	Temporal	3,3

Table 2. Chemical shifts of main metabolites observed in OPCs

Metabolite	δ (ppm), multiplicity, number H
myo-inositol	3.93, m
myo-inositol	3.77, m
glycine	3.54, s 2H
taurine	3.42, t, 2H
hipotaurine	3.30, t, 2H
total-choline	3.23, s, 9H
glutamine	2.44, m, 2H
glutamate	2.34, m, 2H
glutamine/glutamate/NAA	2.12
acetate	1.91, s, 3H
lipids	1.70
alanine	1.47, d, 3H
lactate and lipids (methylene)	1.31
lipids and aminoacids (methyl)	0.94, t, 3H

Table 3: Analysis of OPCs migration. The table shows the number of stops of migrating OPCs expressed as: number of stops/number of analyzed cells, in control conditions and in the presence of FGF2 and anosmin-1.

	CONDITION		
Specie and age	**CT**	**FGF2**	**Anosmin-1**
Mouse P0	6.2	3.5	0.85
Mouse P15	11.4	1.52	20.7
Mouse P60	3.76	2.63	8.42
Non tumoral human, adult	3.61	8.8	17.6
Tumoral human, adult	23.7	19.7	23.1

Figure 1

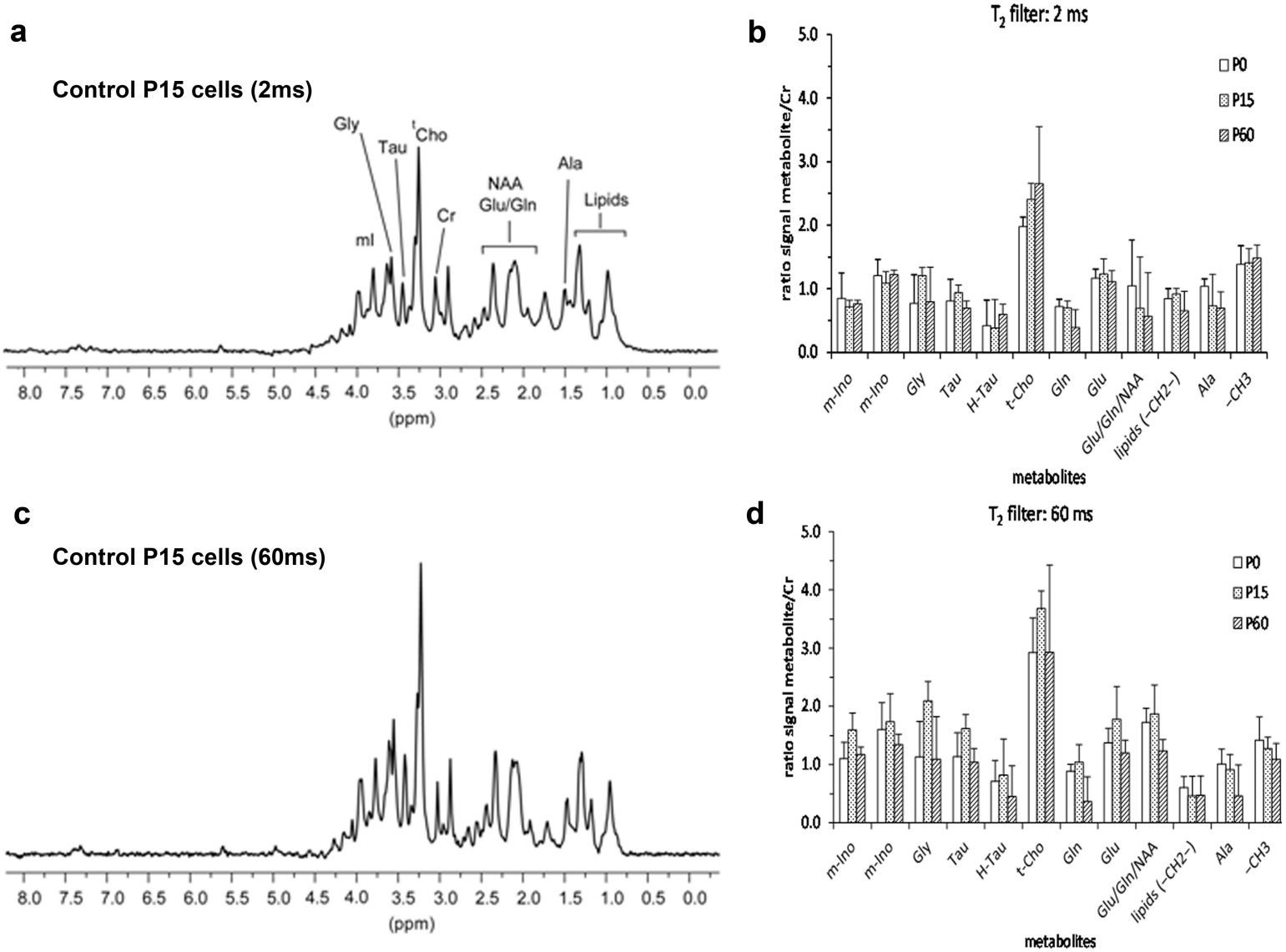
a
Control P15 cells (2ms)
Gly
Tau
tCho
mI
Cr
NAA
Glu/Gln
Ala
Lipids
8.0 7.5 7.0 6.5 6.0 5.5 5.0 4.5 4.0 3.5 3.0 2.5 2.0 1.5 1.0 0.5 0.0
(ppm)
b
T2 filter: 2 ms
ratio signal metabolite/Cr
5.0
4.0
3.0
2.0
1.0
0.0
P0
P15
P60
m-Ino
m-Ino
Gly
Tau
H-Tau
t-Cho
Gln
Glu
Glu/Gln/NAA
lipids (–CH2–)
Ala
–CH3
metabolites
c
Control P15 cells (60ms)
8.0 7.5 7.0 6.5 6.0 5.5 5.0 4.5 4.0 3.5 3.0 2.5 2.0 1.5 1.0 0.5 0.0
(ppm)
d
T2 filter: 60 ms
ratio signal metabolite/Cr
5.0
4.0
3.0
2.0
1.0
0.0
P0
P15
P60
m-Ino
m-Ino
Gly
Tau
H-Tau
t-Cho
Gln
Glu
Glu/Gln/NAA
lipids (–CH2–)
Ala
–CH3
metabolites

Figure 2

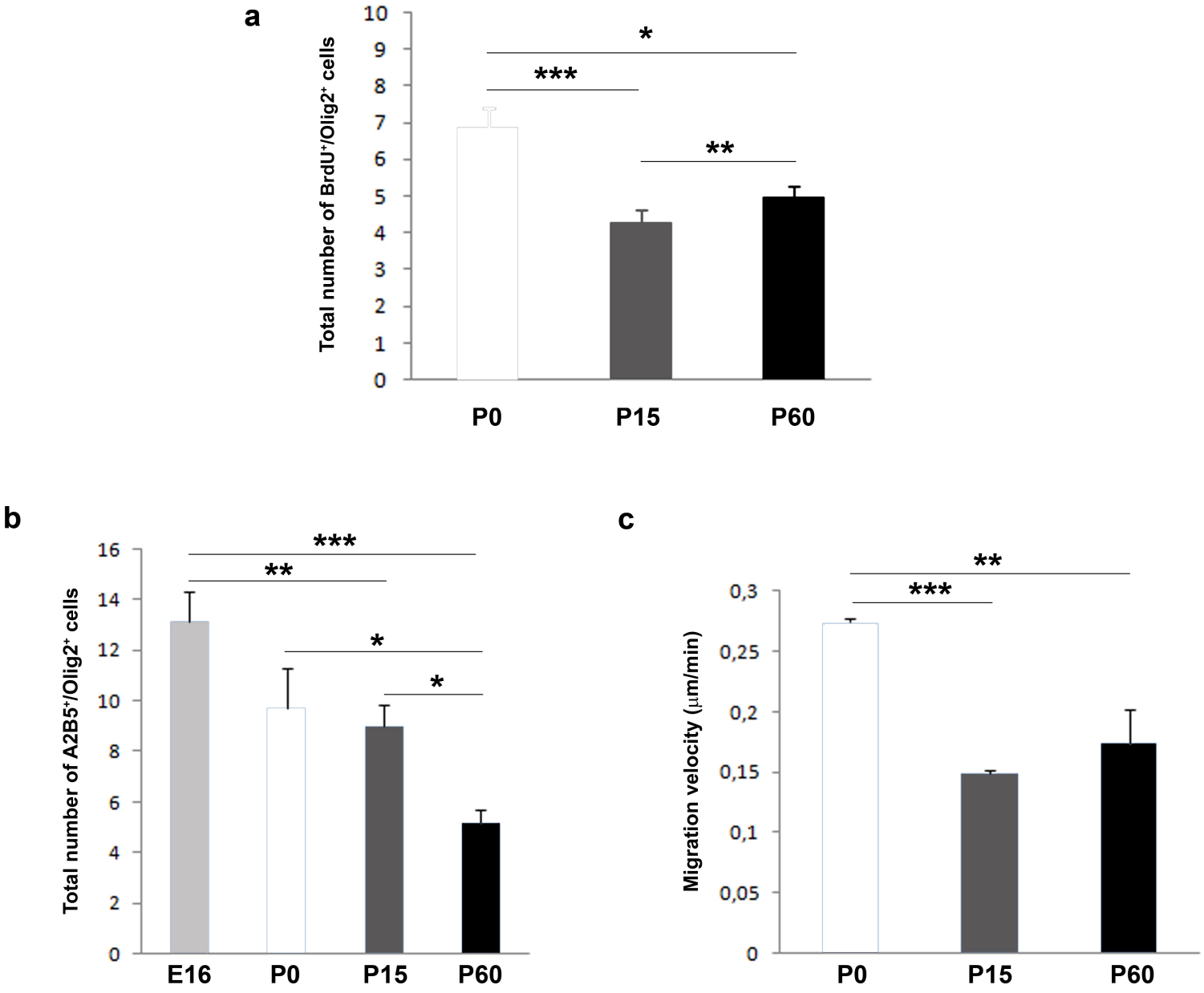
a
Total number of BrdU+/Olig2+ cells
10
9
8
7
6
5
4
3
2
1
0
*
***
**
P0
P15
P60
b
Total number of A2B5+/Olig2+ cells
16
14
12
10
8
6
4
2
0
***
**
*
*
E16
P0
P15
P60
c
Migration velocity (µm/min)
0,3
0,25
0,2
0,15
0,1
0,05
0
**
***
P0
P15
P60

Figure 3

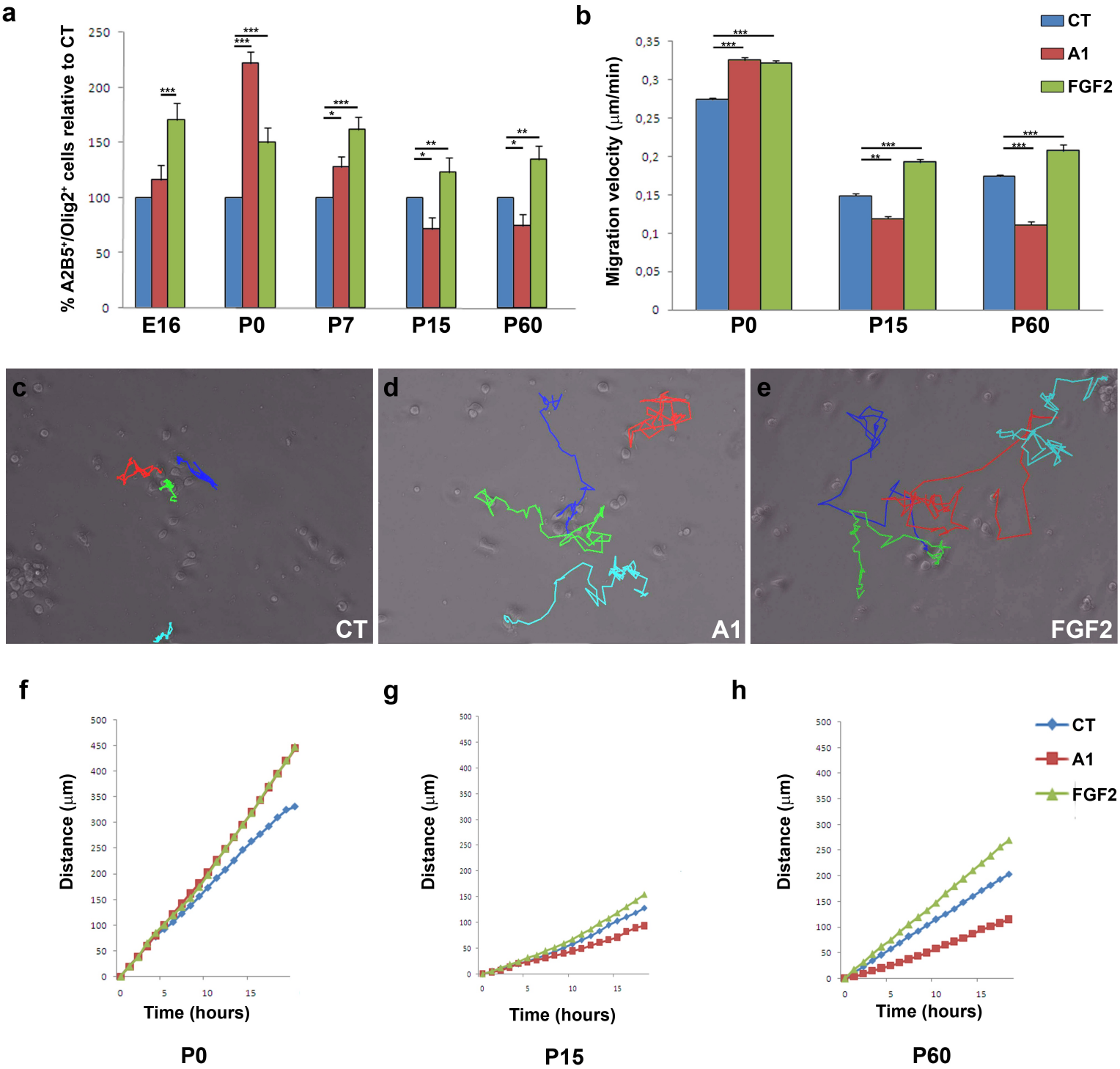
a
% A2B5+/Olig2+ cells relative to CT
250
200
150
100
50
0
E16
P0
P7
P15
P60
b
Migration velocity (µm/min)
0,35
0,3
0,25
0,2
0,15
0,1
0,05
0
P0
P15
P60
CT
A1
FGF2
c
CT
d
A1
e
FGF2
f
Distance (µm)
Time (hours)
P0
g
Distance (µm)
Time (hours)
P15
h
Distance (µm)
Time (hours)
P60
CT
A1
FGF2

Figure 4

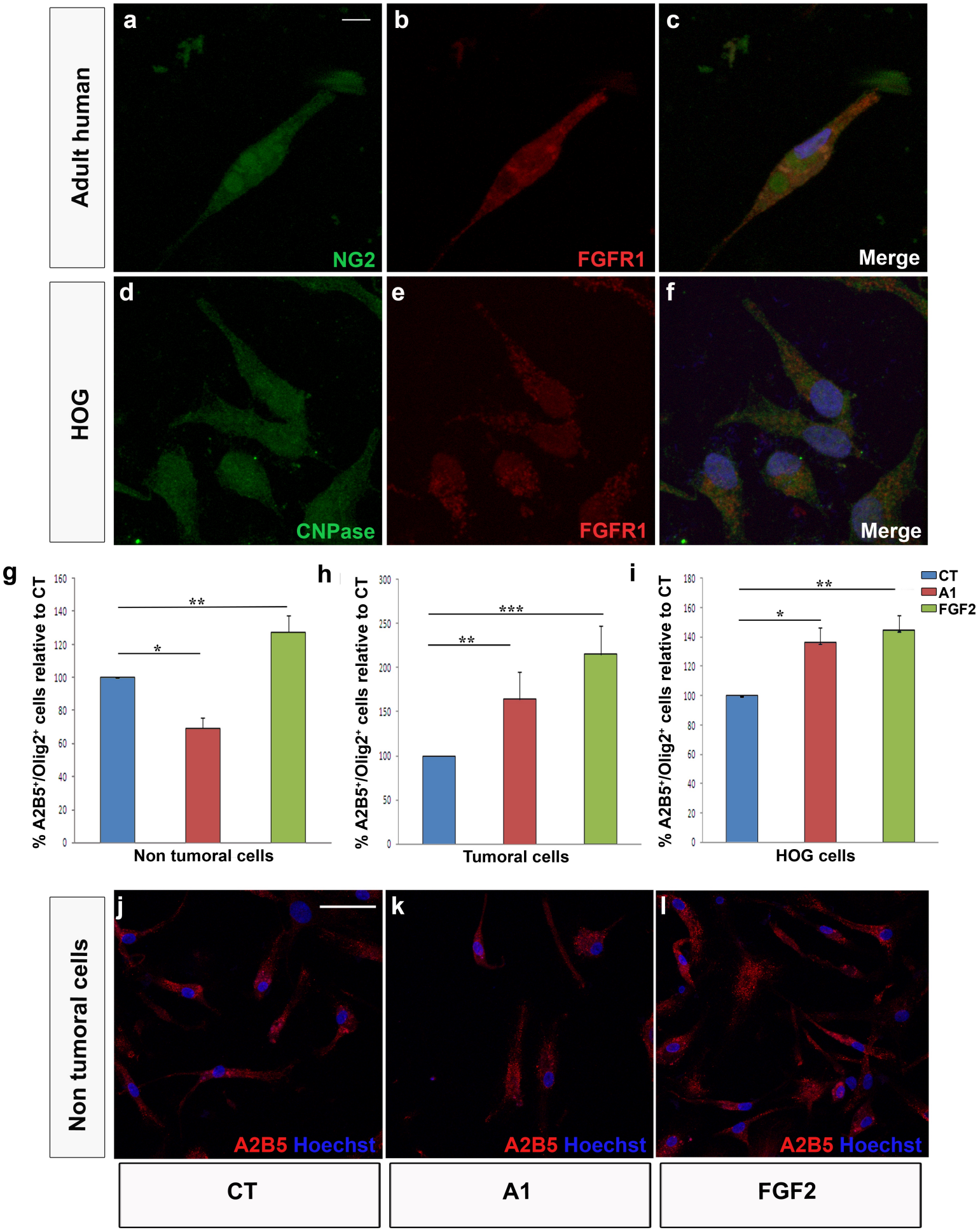
Adult human
a
NG2
b
FGFR1
c
Merge
HOG
d
CNPase
e
FGFR1
f
Merge
g
% A2B5+/Olig2+ cells relative to CT
Non tumoral cells
h
% A2B5+/Olig2+ cells relative to CT
Tumoral cells
i
% A2B5+/Olig2+ cells relative to CT
HOG cells
CT
A1
FGF2
Non tumoral cells
j
A2B5 Hoechst
k
A2B5 Hoechst
l
A2B5 Hoechst
CT
A1
FGF2

Figure 5

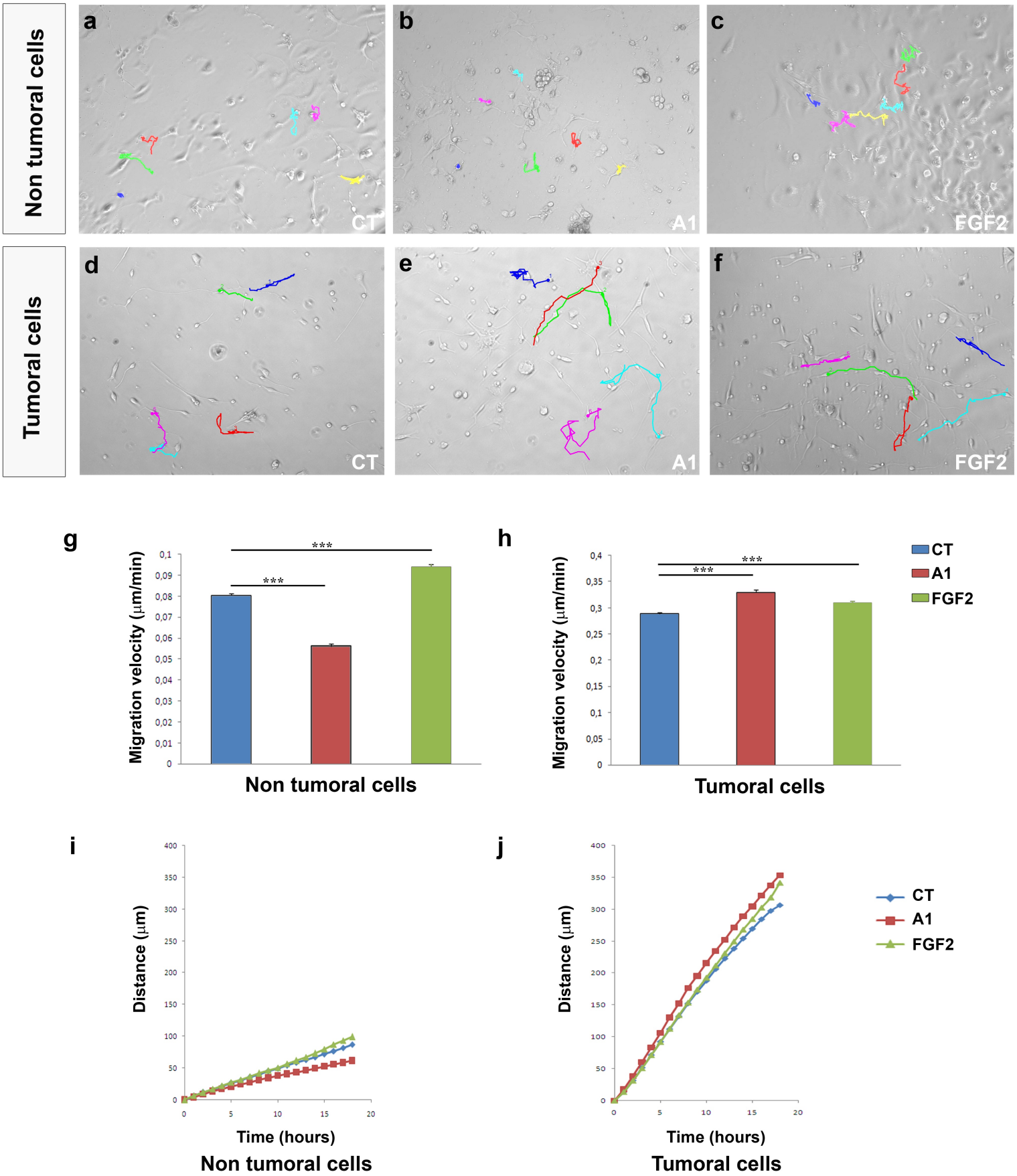
Non tumoral cells
Tumoral cells
a
b
c
d
e
f
CT
A1
FGF2
g
h
Migration velocity (µm/min)
***
Non tumoral cells
Tumoral cells
CT
A1
FGF2
i
j
Distance (µm)
Time (hours)
Non tumoral cells
Tumoral cells

Figure 6

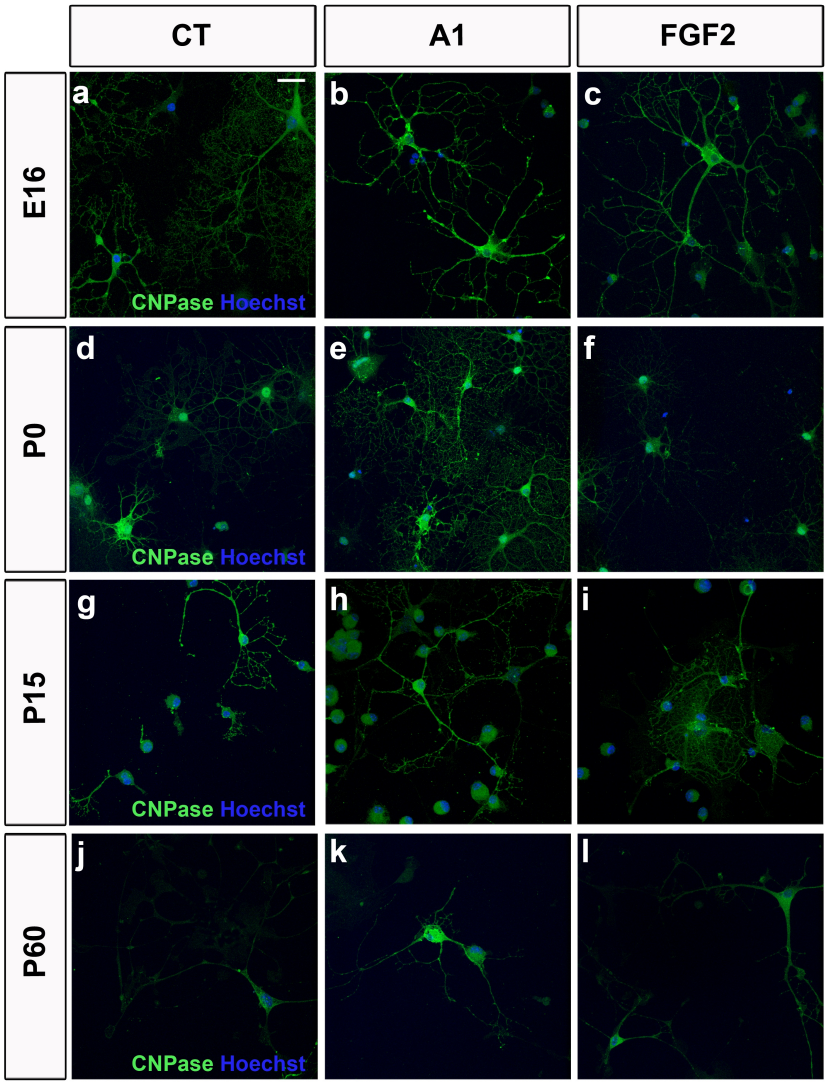
CT
A1
FGF2
E16
P0
P15
P60
a
b
c
d
e
f
g
h
i
j
k
l
CNPase Hoechst

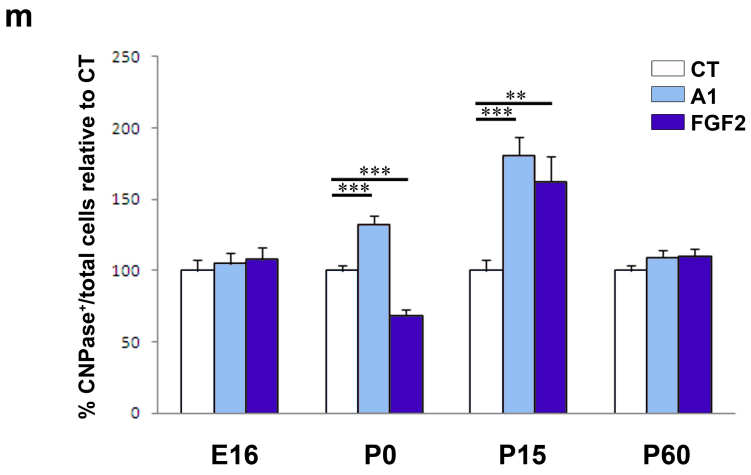
m
% CNPase+/total cells relative to CT
250
200
150
100
50
0
CT
A1
FGF2
***
***
**
***
E16
P0
P15
P60

Figure 7

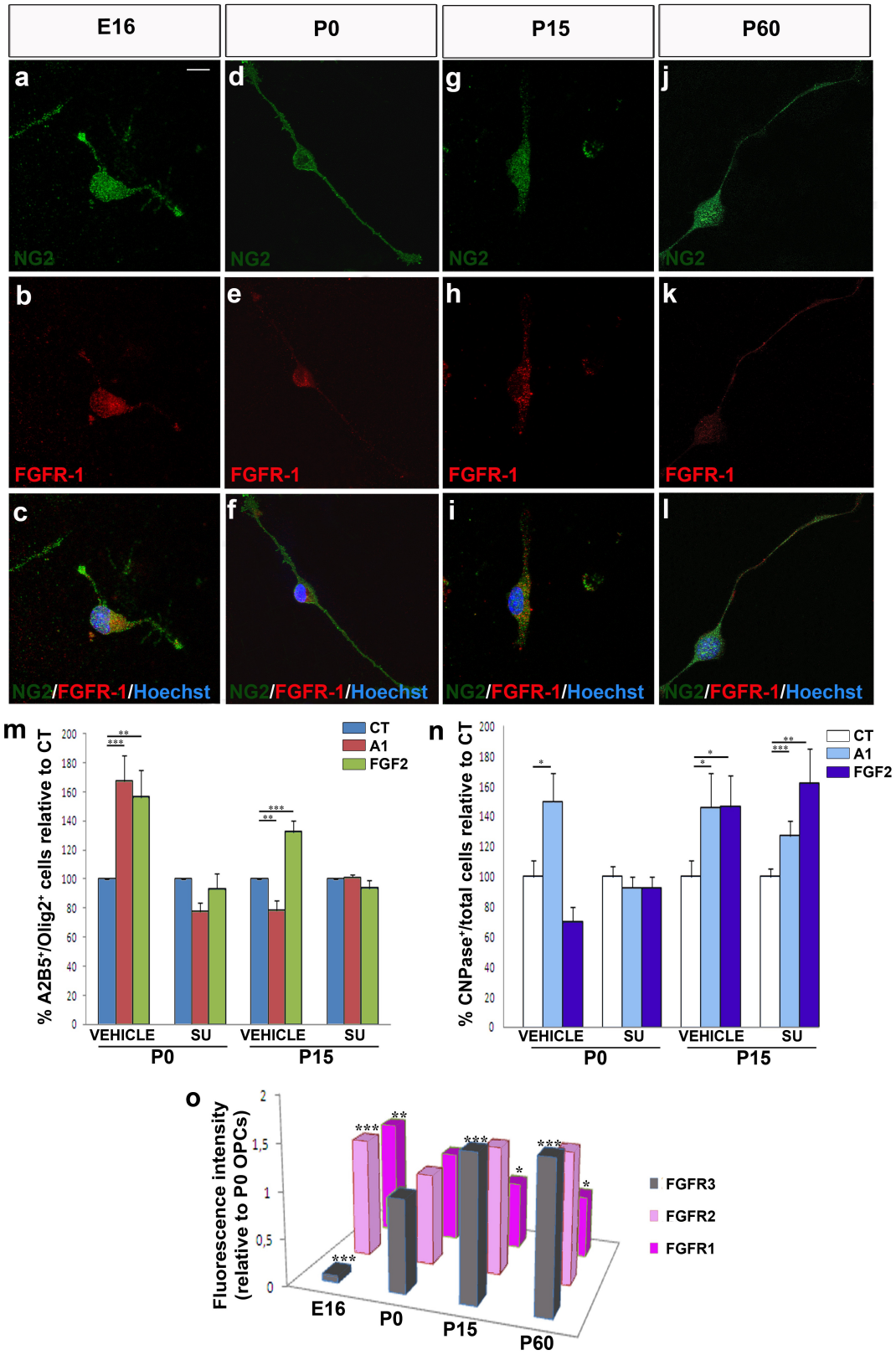
E16
P0
P15
P60
a
d
g
j
NG2
b
e
h
k
FGFR-1
c
f
i
l
NG2/FGFR-1/Hoechst
m
% A2B5+/Olig2+ cells relative to CT
CT
A1
FGF2
VEHICLE
SU
VEHICLE
SU
P0
P15
n
% CNPase+/total cells relative to CT
CT
A1
FGF2
VEHICLE
SU
VEHICLE
SU
P0
P15
o
Fluorescence intensity (relative to P0 OPCs)
FGFR3
FGFR2
FGFR1
E16
P0
P15
P60